SUPPLEMENTARY MATERIALS

Elasticity and Thermal Stability are Key Determinants of Hearing Rescue by Mini-Protocadherin-15 Proteins

Pedro De-la-Torre[1,†], Haosheng Wen[2,3,&,†], Joseph Brower[1], Karina Martínez-Pérez[1,4], Yoshie Narui[5], Frank Yeh[1], Evan Hale[1], Maryna V. Ivanchenko[6], David P. Corey[6], Marcos Sotomayor[2,3,&,*], Artur A. Indzhykulian[1,*].

[1] Department of Otolaryngology - Head and Neck Surgery, Harvard Medical School and Massachusetts Eye and Ear, 243 Charles St, Boston, MA, USA

[2] Department of Chemistry and Biochemistry, The Ohio State University, 484 W. 12th Avenue, Columbus, OH, USA.

[3] Biophysics Program, The Ohio State University, 484 W. 12th Avenue, Columbus, OH, USA.

[4] Biology Program, Department of Basic Sciences, Universidad del Atlántico, Cra 30 # 8-49, Puerto Colombia, 081007, Colombia.

[5] Center for Electron Microscopy and Analysis, The Ohio State University, 1275-1305 Kinnear Road, Columbus, OH, USA.

[6] Department of Neurobiology, Harvard Medical School, 200 Longwood Ave, Boston, MA, USA

[7] Speech and Hearing Biosciences and Technology graduate program, Harvard University, Cambridge, MA, USA.

[&] Current address: Department of Biochemistry and Molecular Biology, The University of Chicago, 929 E 57th St, Chicago, IL, USA.

*Corresponse should be addressed to inartur@hms.harvard.edu and sotomayor@uchicago.edua

[†]These authors contributed equally to this work

SUPPLEMENTARY DISCUSSION

Assignment and equilibrium dynamics of Ca^{2+} bound to engineered linkers in mini-PCDH15 models

Our AlphaFold2 (AF2) and aligned (AL) models of mini-PCDH15 ectodomains included engineered linker regions where we manually placed bound Ca^{2+} ions. Mini-PCDH15-V4 **(Fig. 4a, 4d)** has one engineered EC3-EC9 linker region with the atypical p.366DENNQ linker motif. The native EC3-EC4 linker region with this motif and with Ca^{2+} observed at sites 2 and 3 [79] exhibits reduced Ca^{2+} binding ability compared to what is expected for linker regions with the canonical DXNDN Ca^{2+} binding motif and three bound Ca^{2+}. Analysis of our EC3-EC9 AF2 and AL models **(Fig. 4 and S3)**, revealed residues arranged in conformations that were compatible with Ca^{2+} binding at sites 2 and 3, where Ca^{2+} ions were placed **(Fig. 4b** and **4e**, *left middle* panels**)**. Interestingly, Ca^{2+} at site 2 was coordinated by p.N369 in the mini-PCDH15-V4 AL model, but not in the mini-PCDH15-V4 AF2 model. Mini-PCDH15-V4 AF2 and AL models showed consistent Ca^{2+} coordination profiles pre- and post-simulation **(Fig. 4b** and **4e**, *right middle* panels**)**.

Mini-PCDH15-V7 **(Fig. 4g** and **4j)** features two engineered linker regions: EC3-EC7 and EC8-EC11. The EC3-EC7 linker region has the non-canonical p.366DENNQ linker motif. Our AF2 model **(Fig. 4h**, *left middle*), the AL model **(Fig. 4k**, *left middle)*, and the crystal structure **(Fig. 3a)** show a Ca^{2+} bound at site 3, as expected. Notably, our crystal structure of the EC3-EC7 fragment has a K^{+} at site 1, with no cation occupancy at site 2 **(Fig. 3a)**. In contrast, in both the AF2 and the AL models, Ca^{2+} ions were placed at site 2, leading to p.D724 coordinating Ca^{2+} ions at sites 2 and 3, as we previously observed in the native EC3-EC4 linker with residue p.D411 (PDB: 5T4M). In both the AF2 and AL models, the side chains of the linker motif segment p.368NNQ are oriented in a configuration consistent with the EC3-4 crystal structure **(Fig. 3a**, **Fig. 4h** and **4k**, *left middle*). Equilibrium simulations also revealed that in both models for mini-PCDH15-V7 EC3-EC7, the backbone oxygen atom of p.N728 loses coordination with the Ca^{2+} ion at site 3 (**Fig. 4h** and **4k**, *right middle*), inconsistent with the configuration observed in the EC3-EC7 crystal structure (**Fig. 3a**). In contrast, Ca^{2+} at site 2 moved close to site 1 during the equilibration of the AL model, to a position that is consistent with that observed for K^{+} in the crystal structure **(Fig. 3a)**.

Our models for the engineered linker region EC8-EC11 of mini-PCDH15-V7 with the p.897DMNDY linker motif, display similar Ca^{2+} coordination at sites 2 and 3 pre- and post-simulation (**Fig. S3b** and **S3e**, middle panels). However, the backbone oxygen atom of p.Y1155 loses its coordination with the Ca^{2+} ion at site 3 after equilibration (**Fig. S3b** and **S3e**, *right middle* panels).

Models for mini-PCDH15-V8 and its engineered EC4-EC7 **(Fig. S3g and S3j)** linker region with the canonical p.480DANDN linker motif displayed Ca^{2+} coordination at sites 2 and 3 (**Fig. S3h** and **S3k**, *left* panels), similar to that observed in our crystal structure **(Fig. 3b)**. Post-simulation, however, both models exhibited a notable shift: the backbone oxygen atom of p.N728 moved away from the Ca^{2+} ion at site 3 (**Fig. S3h** and **S3k**, *right middle*

panels), accompanied by a general increase in flexibility **(Fig. S3i** and **S3l)**. Furthermore, our AF2 and AL models of the engineered EC7-EC11 linker region with a canonical p.790DIDDN linker motif had identical Ca^{2+} binding configurations **(Fig. 4n** and **4q)**. Equilibrium simulations of mini-PCDH15-V8 AF2 and AL models revealed a consistent pattern: the backbone oxygen atom at p.Y1155 disengaged from the Ca^{2+} ion at site 3 in both models (**Fig. 4n** and **4q**, *right middle* panels), although the overall Ca^{2+} coordination remained unchanged pre- and post-simulation.

Supplementary Figures and Tables

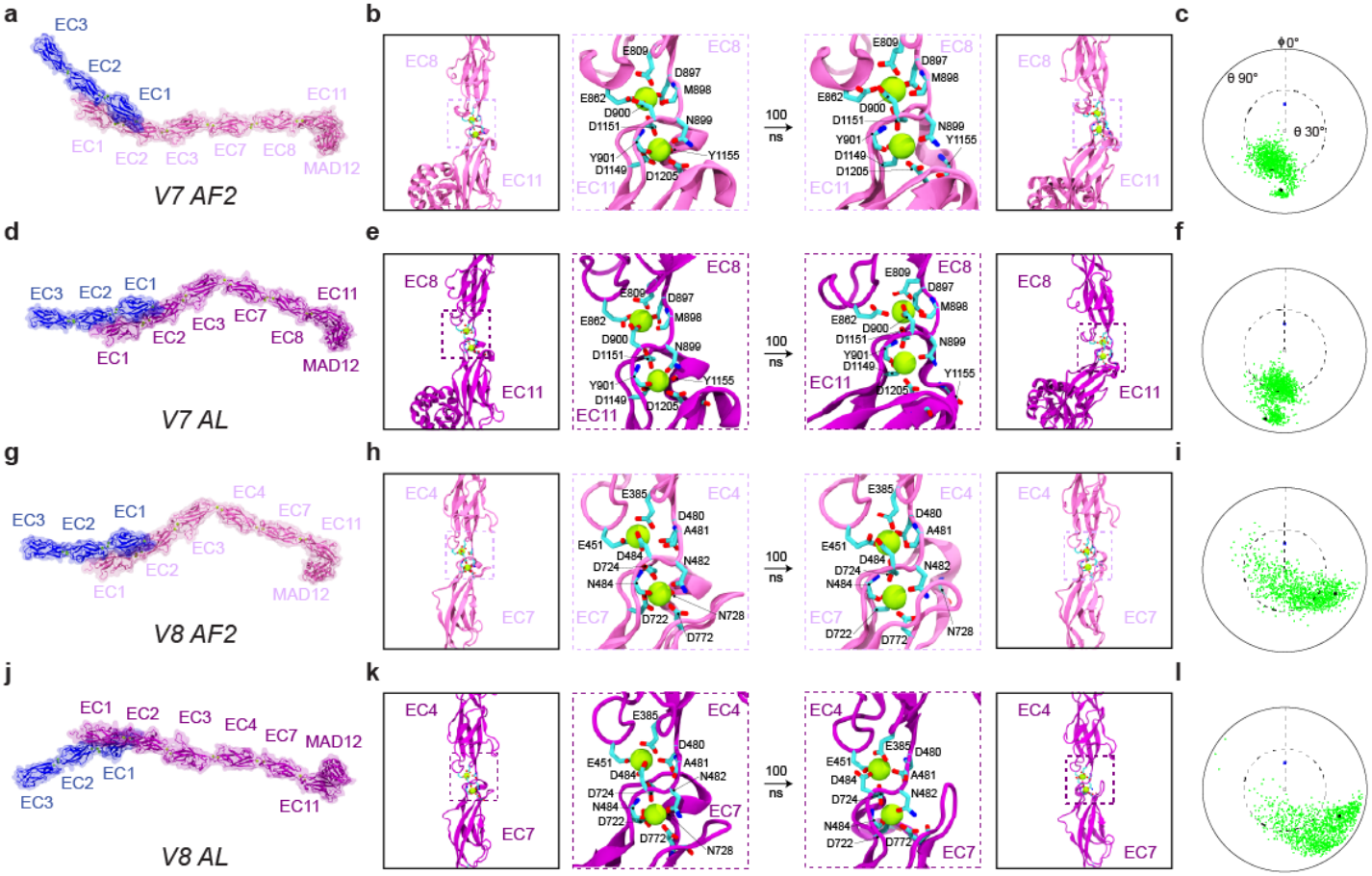

Fig. S1 | Structural models and equilibrium MD simulations of mini-PCDH15-V7 and -V8. a, Full ectodomain of mini-PCDH15-V7 AF2. **b**, Views of the EC8-EC11 linker region at beginning and end of 100-ns MD equilibrations. **c**, Inter-repeat linker flexibility of EC8-EC11 repeats in mini-PCDH15-V7 AF2 (as in **Fig. 5c**). **d,** Full ectodomain of mini-PCDH15-V7 AL. **e**, Views of EC8-EC11 in mini-PCDH15-V7 AL (as in **Fig. 5b**). **f**, Inter-repeat linker flexibility (as in **Fig. 5c**) of EC8-EC11 repeats in mini-PCDH15-V7 AL. **g**, Full ectodomain of mini-PCDH15-V8 AF2. **h**, Views of EC4-EC7 in mini-PCDH15-V8 AF2 (as in **Fig. 5b**). **i**, Inter-repeat linker flexibility (as in **Fig. 5c**) of EC4-EC7 in mini-PCDH15-V8 AF2. **j**, Full ectodomain of the mini-PCDH15-V8 AL. **k**, Views of EC4-EC7 in mini-PCDH15-V8 AL (as in **Fig. 5b**). **l**, Inter-repeat linker flexibility (as in **Fig. 5c**) of EC4-EC7 in mini-PCDH15-V8 AL. All molecular images display protein backbones in cartoon and sidechains in sticks. Mini-PCDH15 proteins with AF2-predicted engineered linker regions are shown in mauve, whereas those assembled based on alignments (AL) are in purple.

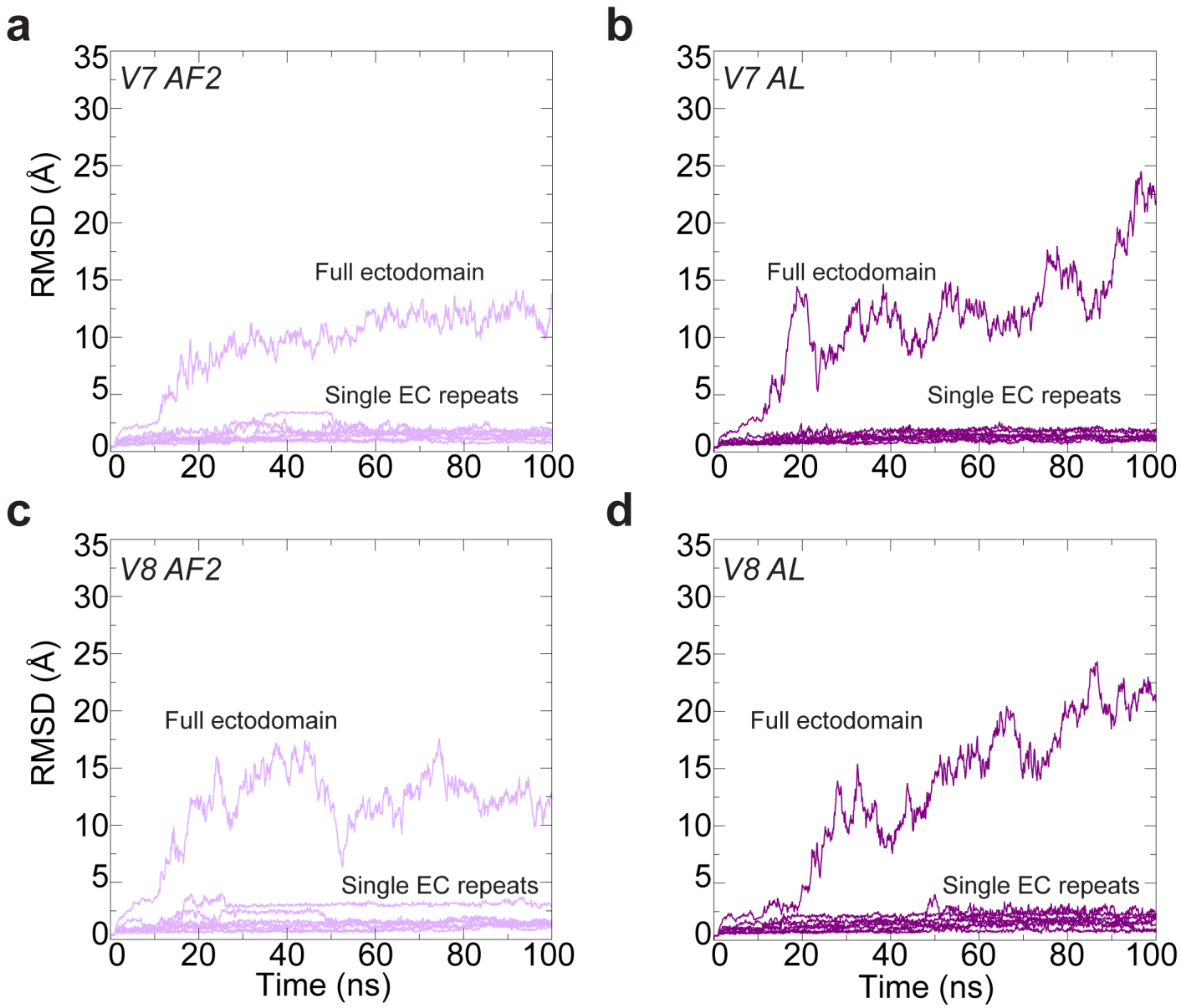

Fig. S2 | Structural stability of mini-PCDH15s. a-d, Root-mean-square deviation (RMSD) as a function of time for the full ectodomains and individual EC repeats of the mini-PCDH15-V7 and -V8 AF2 and AL models.

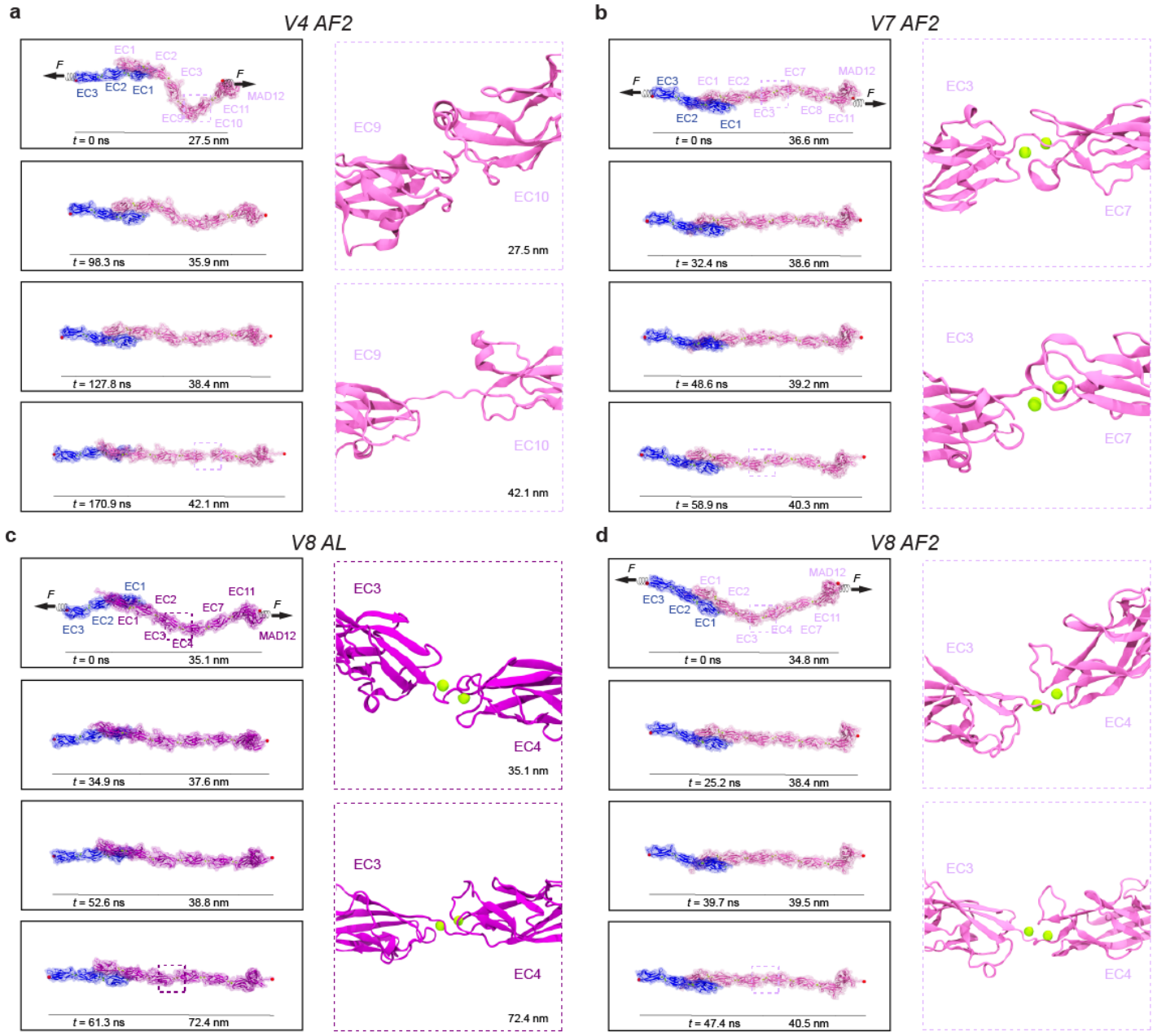

Fig. S3 | Elasticity of monomeric mini-PCDH15 proteins in complex with CDH23 EC1-3. a, Snapshots of mini-PCDH15-V4 AF2 + CDH23 EC1-3 during stretching at 0.1 nm/ns (Sim1d). C-terminal Cα atoms are shown as red spheres. Applied forces are indicated with spring arrows. Insets highlight the most extended EC linker (EC9-EC10). **b**, Snapshots of mini-PCDH15-V7 AF2 + CDH23 EC1-3 during stretching at 0.1 nm/ns (Sim3d). **c**, Snapshots of mini-PCDH15-V8 AL + CDH23 EC1-3 during stretching at 0.1 nm/ns (Sim6d). **d**, Snapshots of mini-PCDH15-V8 AF2 + CDH23 EC1-3 during stretching at 0.1 nm/ns (Sim5d).

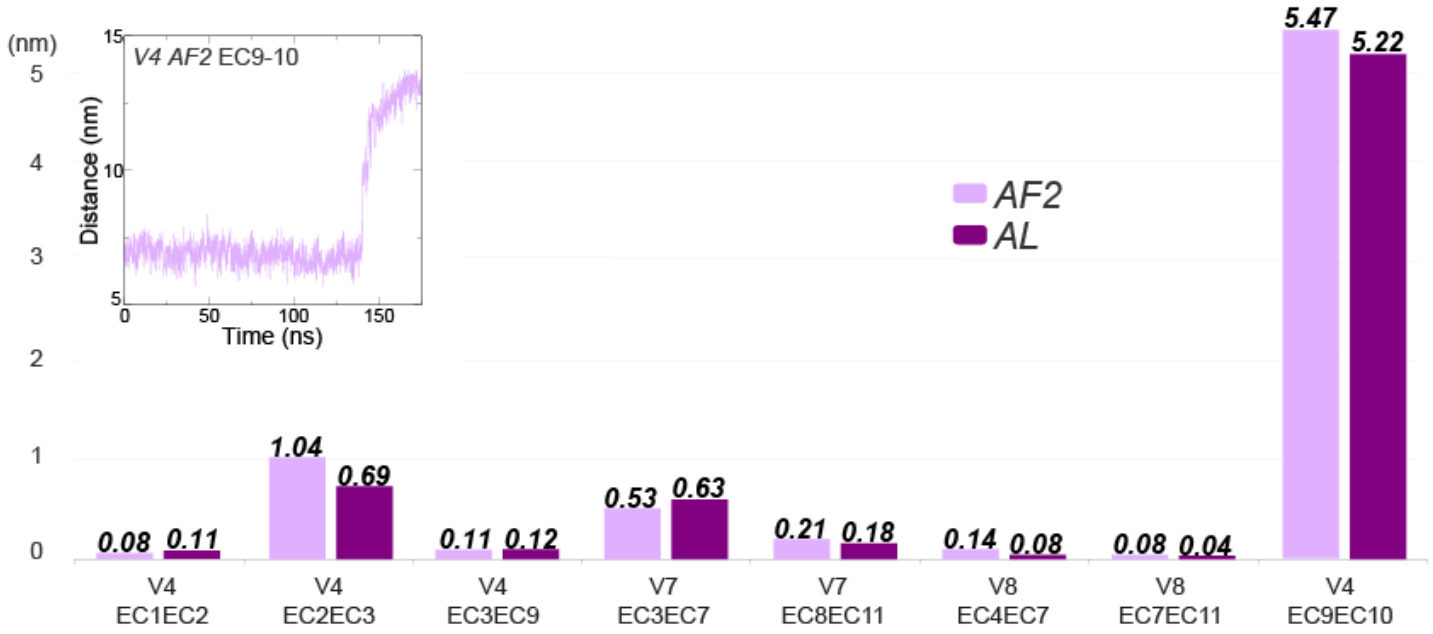

Fig. S4 | Extension of mini-PCDH15 linker regions in stretching simulations at 0.1 nm/ns. The linker regions are depicted based on two different models: AF2 predictions shown in mauve and AL predictions in purple.

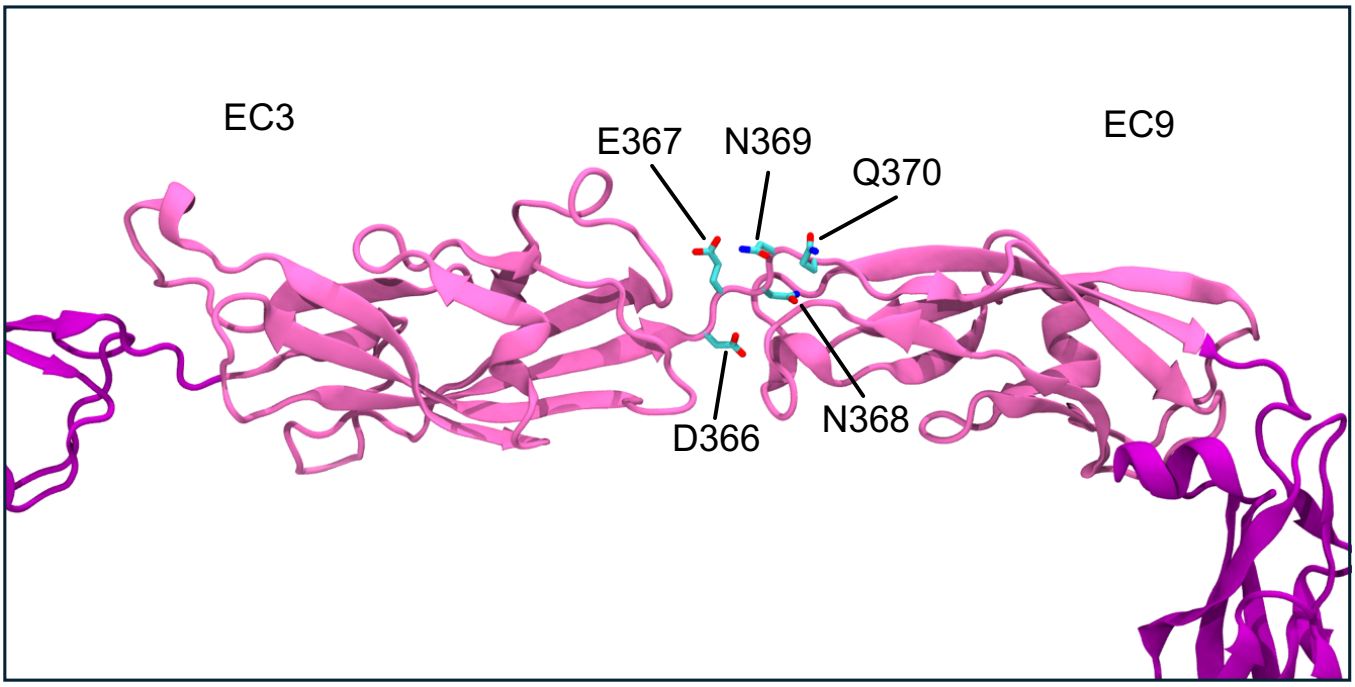

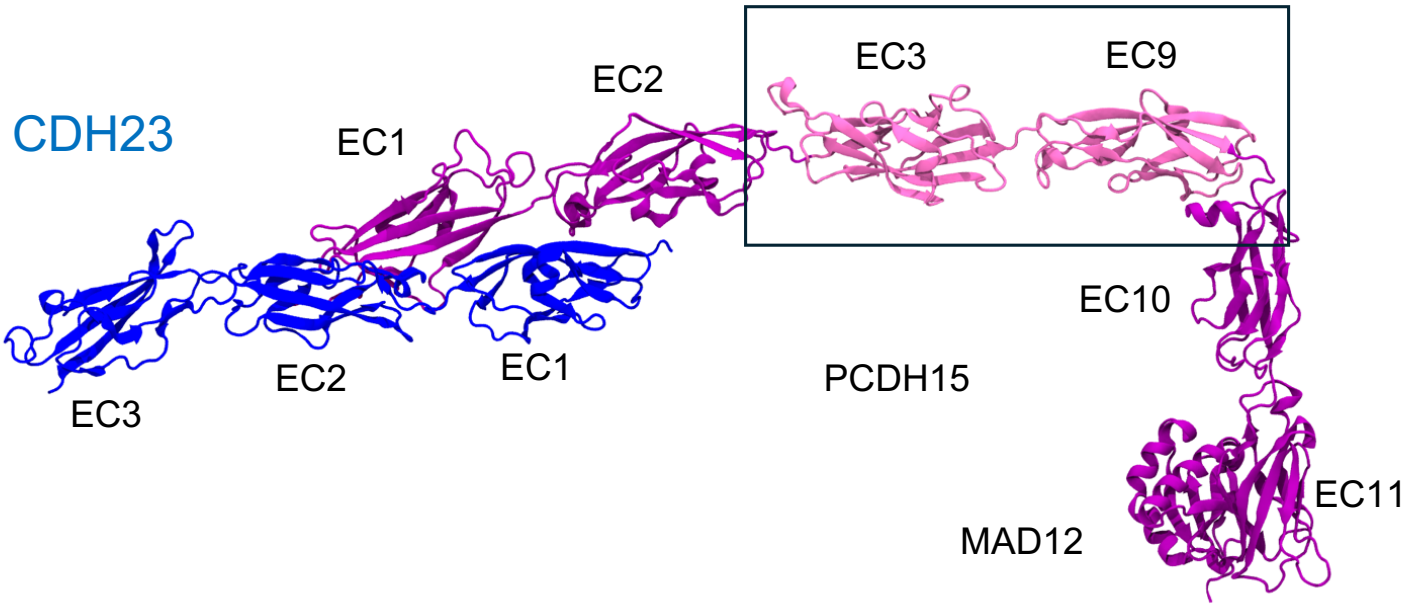

Fig. S5 | **Assembly of mini-PCDH15-V4 AF2 model**. Base model from Choudhary et al. includes CDH23 EC1-3 in blue, PCDH15 EC1-2 in purple, and PCDH15 EC10-MAD12 in purple. Engineered linker EC3-EC9 (in mauve) was predicted using AF2. We then manually connected the C-terminal end of PCDH15 EC1-2 to the N-terminal end of the AF2-predicted PCDH15 EC3-EC9. Similarly, the C-terminal end of the AF2-predicted EC3-EC9 was connected to N-terminal end of PCDH15 EC10-MAD12. Box highlights the AF2-predicted EC3-EC9 subdomain.

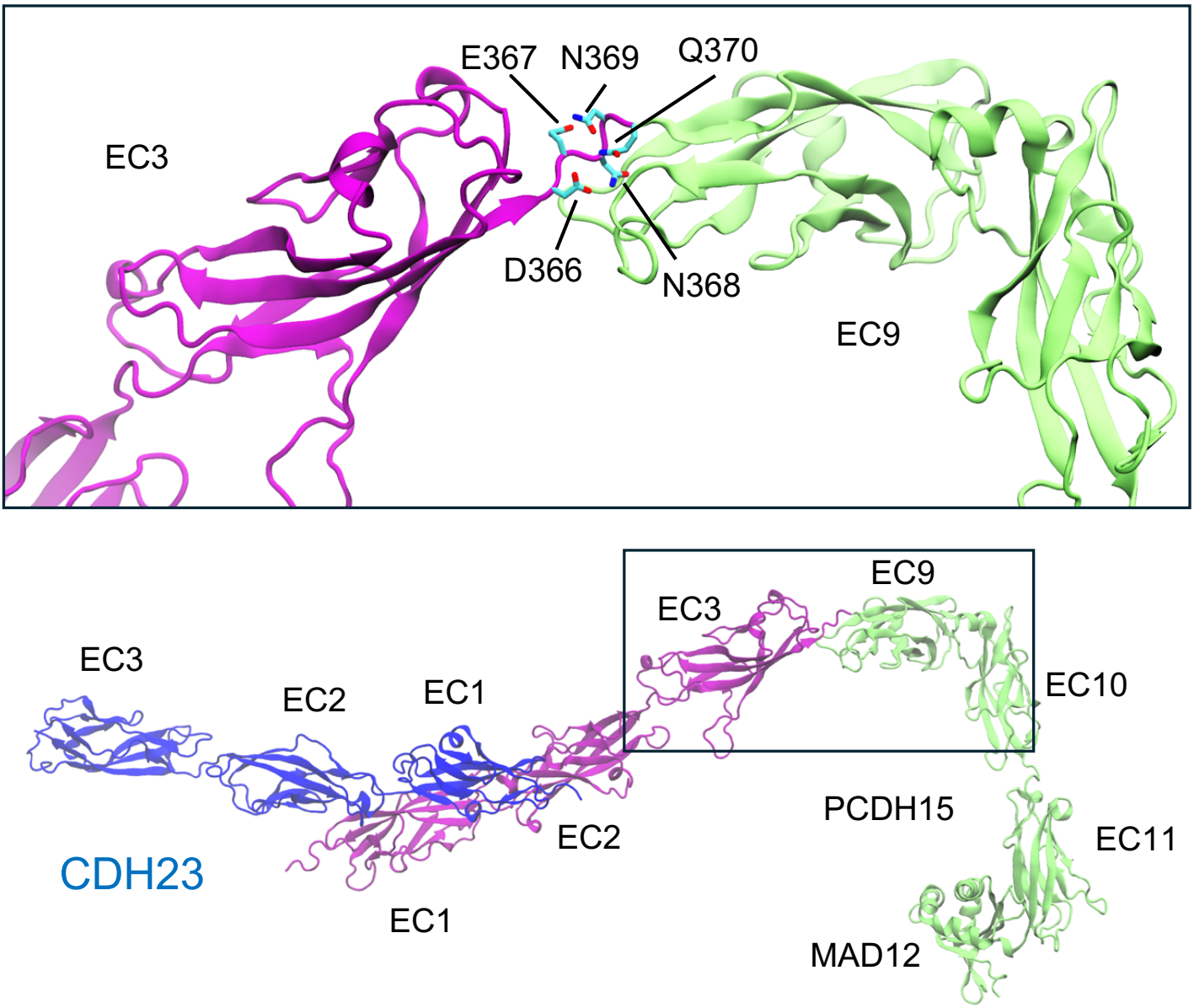

Fig. S6 | **Assembly of mini-PCDH15-V4 AL model**. Base model from Choudhary et al. includes CDH23 EC1-3 in blue, PCDH15 EC1-3 in purple, and PCDH15 EC9-MAD12 in lime. We manually connected the C-terminal end of PCDH15 EC1-3 to the N-terminal end of PCDH15 EC9-MAD12. Box highlights the engineered linker region.

Table S1 | RMSD values from COOT using atoms of protein backbone between PDB structures of linkers and WT domains (Å)

	8TON EC3	8UMZ EC4 (chain A)	8UMZ EC4 (chain B)	8TON EC7	8UMZ EC7 (chain A)	8UMZ EC7 (chain B)
5T4M EC3 (chain A)	1.083	-	-	-	-	-
5T4M EC3 (chain B)	0.842	-	-	-	-	-
5T4M EC4 (chain A)	-	0.925	0.395	-	-	-
5T4M EC4 (chain B)	-	0.395	0.473	-	-	-
5ULY EC3	0.511	-	-	-	-	-
5W1D EC4	-	0.729	0.719	-	-	-
5W1D EC7	-	-	-	0.516	0.594	0.649
6BWN EC7	-	-	-	0.399	0.435	0.533

Table S2 | Summary of simulations for mini-PCDH15 proteins + CDH23 EC1-3.

Label	System	t_{sim} (ns)	Type	Start	Speed (nm/ns)	Average force Peak (pN)	Size (#atoms)	Initial Sytem Size (nm^3)
Sim1a	V4 AF2	100	EQ	-	-	-	1,239,195	76×14×12
Sim1b		1.24	SMD	S1a	10	695.0 +/- 197.8		
Sim1c		9.85	SMD	S1a	1	388.4 +/- 23.0		
Sim1d		170.9	SMD	S1a	0.1	355.8 +/- 12.7		
Sim2a	V4 AL	100	EQ	-	-	-	938,545	76×16×8
Sim2b		1.2	SMD	S2a	10	713.5 +/- 261.7		
Sim2c		9.77	SMD	S2a	1	390.7 +/- 51.2		
Sim2d		189.2	SMD	S2a	0.1	315.1 +/- 0.6		
Sim3a	V7 AF2	100	EQ	-	-	-	1,060,405	76×12×12
Sim3b		0.94	SMD	S3a	10	754.4 +/- 236.0		
Sim3c		6.74	SMD	S3a	1	431.9 +/- 49.0		
Sim3d		84.0	SMD	S3a	0.1	291.8 +/- 48.8		
Sim4a	V7 AL	100	EQ	-	-	-	1,060,492	76×12×12
Sim4b		0.98	SMD	S4a	10	729.5 +/- 236.2		
Sim4c		6.35	SMD	S4a	1	411.9 +/- 55.9		
Sim4d		100.6	SMD	S4a	0.1	287.2 +/- 4.0		
Sim5a	V8 AF2	100	EQ	-	-	-	1,060,357	76×12×12
Sim5b		0.96	SMD	S5a	10	753.8 +/- 204.0		
Sim5c		6.16	SMD	S5a	1	402.9 +/- 65.7		
Sim5d		84.5	SMD	S5a	0.1	353.3 +/- 41.2		
Sim6a	V8 AL	100	EQ	-	-	-	1,060,501	76×12×12
Sim6b		0.96	SMD	S6a	10	731.3 +/- 204.8		
Sim6c		6.25	SMD	S6a	1	388.7 +/- 68.2		
Sim6d		84.1	SMD	S6a	0.1	309.7 +/- 7.7		

Table S3 | Predicted elasticity of monomeric mini-PCDH15 proteins

Mini-PCDH15 Versions	Effective Spring Constant *k* (mN/m)		Extensibility (nm)	
V4 AF2	3.3	34.2	9.0	5.0
V4 AL	3.3	17.2	7.0	7.5
V7 AF2	36.3		4.5	
V7 AL	33.0		5.5	
V8 AF2	53.9		3.5	
V7 AL	55.5		4.0	

Table S4 | RMSD values between AF2 and AF3 predictions for mini-PCDH15 engineered linkers

Mini-PCDH15 Engineered linkers	RMSD Values Using Non-Hydrohen Atoms (Å)	RMSD Values Using Atoms of Protein Backbone (Å)
V4 AF2 EC3	2.359	1.166
V4 AF2 EC3-EC9 linker	2.555	0.698
V4 AF2 EC9	1.773	0.441
V7 AF2 EC3	2.236	0.943
V7 AF2 EC3-EC7 linker	1.779	0.083
V7 AF2 EC7	1.815	0.189
V7 AF2 EC7-EC8 linker	1.662	0.069
V7 AF2 EC8	1.779	0.314
V7 AF2 EC8-EC11 linker	1.489	0.071
V7 AF2 EC11	2.661	1.005
V8 AF2 EC4	1.721	0.192
V8 AF2 EC4-EC7 linker	1.798	0.103
V8 AF2 EC7	1.752	0.122
V8 AF2 EC7-EC11 linker	1.649	0.091
V8 AF2 EC11	3.221	1.714

Movies

Movie S1. Animation of 2D class averages of mini-PCDH15-V4 demonstrating the various conformations present.

Movie S2. Forced unbending and unrolling in a simulation of the mini-PCDH15 V4 AF2 (EC1-EC2-EC3-EC9-EC10-EC11-MAD12 in mauve) + CDH23 (EC1-3 in blue) model. Stretching of the complex at 0.1 nm/ns (simulation s1d in SI Appendix, Table S1, 0 - 170.9 ns) results in straightening of the mini-PCDH15 V4 AF2 ectodomain with lengthening of the EC2-3 and EC9-10 linker regions. As the simulation progresses the mini-PCDH15 MAD12 began to unfold from its C-terminal end. The mini-PCDH15 MAD12 eventually unrolled away from EC11 while unfolding continued. The CDH23 EC1-3 did not unbind from mini-PCDH15 V4 AF2.

Movie S3. Forced unbending and unrolling in a simulation of the mini-PCDH15 V4 AL (EC1-EC2-EC3-EC9-EC10-EC11-MAD12 in purple) + CDH23 (EC1-3 in blue) model. Stretching of the complex at 0.1 nm/ns (simulation s2d in SI Appendix, Table S1, 0 - 189.2 ns) results in straightening of the mini-PCDH15 V4 AL ectodomain with lengthening of the EC9-10 linker region. As the simulation progressed the mini-PCDH15 MAD12 began to unfold from its C-terminal end. The mini-PCDH15 MAD12 eventually unrolled away from EC11 while unfolding continued. The CDH23 EC1-3 did not unbind from mini-PCDH15 V4 AL.

Movie S4. Forced unrolling in a simulation of the mini-PCDH15-V7 AF2 (EC1-EC2-EC3-EC7-EC8-EC11-MAD12 in mauve) + CDH23 (EC1-3 in blue) model. Stretching of the complex at 0.1 nm/ns (simulation s3d in SI Appendix, Table S1, 0 - 84.0 ns) results in straightening of the mini-PCDH15-V7 AF2 ectodomains with minimal lengthening of linker regions. As the simulation progressed the mini-PCDH15 MAD12 began to unfold from its C-terminal end. The mini-PCDH15 MAD12s eventually unrolled away from EC11 while unfolding continued. The CDH23 EC1-3 did not unbind from mini-PCDH15 V7 AF2.

Movie S5. Forced unrolling in a simulation of the *mm* (mini-PCDH15-V7 Alignment EC1-EC2-EC3-EC7-EC8-EC11-MAD12 in purple) + (CDH23 EC1-3 in blue) model. Stretching of the complex at 0.1 nm/ns (simulation s4d in SI Appendix, Table S1, 0 - 100.6ns) results in straightening of the mini-PCDH15-V7 Alignment ectodomains with minimal lengthening of linker regions. As the simulation progressed the mini-PCDH15 MAD12s began to unfold from their C-terminal ends. The mini-PCDH15 MAD12s eventually unrolled away from EC11 while unfolding continued. The CDH23 EC1-3 did not unbind from mini-PCDH15 V7 Alignment.

Movie S6. Forced unrolling in a simulation of the *mm* (mini-PCDH15-V8 AlphaFold2 EC1-EC2-EC3-EC4-EC7-EC11-MAD12 in mauve) + (CDH23 EC1-3 in blue) model. Stretching of the complex at 0.1 nm/ns (simulation s5d in SI Appendix, Table S1, 0 - 84.5ns) results in straightening of the mini-PCDH15-V8 AlphaFold2 ectodomains with minimal lengthening of linker regions. As the simulation progressed the mini-PCDH15 MAD12s began to unfold from their C-terminal ends. The mini-PCDH15 MAD12s eventually unrolled away from EC11 while unfolding continued. The CDH23 EC1-3 did not unbind from mini-PCDH15 V8 AlphaFold2.

Movie S7. Forced unrolling in a simulation of the *mm* (mini-PCDH15-V8 Alignment EC1-EC2-EC3-EC4-EC7-EC11-MAD12 in purple) + (CDH23 EC1-3 in blue) model. Stretching of the complex at 0.1 nm/ns (simulation s6d in SI Appendix, Table S1, 0 - 84.1ns) results in straightening of the mini-PCDH15-V8 Alignment ectodomains with minimal lengthening of linker regions. As the simulation progressed the mini-PCDH15 MAD12s began to unfold from their C-terminal ends. The mini-PCDH15 MAD12s eventually unrolled away from EC11 while unfolding continued. The CDH23 EC1-3 did not unbind from mini-PCDH15 V8 Alignment.